

Review

Can the Future EnMAP Mission Contribute to Urban Applications? A Literature Survey

Wieke Heldens ^{1,*}, Uta Heiden ¹, Thomas Esch ¹, Enrico Stein ² and Andreas Müller ¹

¹ Department of Land Applications, German Remote Sensing Data Center, German Aerospace Center, Muenchener Strasse 20, D-82234 Wessling, Germany; E-Mails: uta.heiden@dlr.de (U.H.); thomas.esch@dlr.de (T.E.); andreas.mueller@dlr.de (A.M.)

² Department of Civil Crisis Information and Geo-Risks, German Remote Sensing Data Center, German Aerospace Center, Muenchener Strasse 20, D-82234 Wessling, Germany; E-Mail: enrico.stein@dlr.de

* Author to whom correspondence should be addressed; E-Mail: wieke.heldens@dlr.de; Tel.: +49-8153-28-1190; Fax: +49-8153-28-1458.

Received: 17 June 2011; in revised form: 12 August 2011 / Accepted: 15 August 2011 /

Published: 25 August 2011

Abstract: With urban populations and their footprints growing globally, the need to assess the dynamics of the urban environment increases. Remote sensing is one approach that can analyze these developments quantitatively with respect to spatially and temporally large scale changes. With the 2015 launch of the spaceborne EnMAP mission, a new hyperspectral sensor with high signal-to-noise ratio at medium spatial resolution, and a 21 day global revisit capability will become available. This paper presents the results of a literature survey on existing applications and image analysis techniques in the context of urban remote sensing in order to identify and outline potential contributions of the future EnMAP mission. Regarding urban applications, four frequently addressed topics have been identified: urban development and planning, urban growth assessment, risk and vulnerability assessment and urban climate. The requirements of four application fields and associated image processing techniques used to retrieve desired parameters and create geo-information products have been reviewed. As a result, we identified promising research directions enabling the use of EnMAP for urban studies. First and foremost, research is required to analyze the spectral information content of an EnMAP pixel used to support material-based land cover mapping approaches. This information can subsequently be used to improve urban indicators, such as imperviousness. Second, we identified the global monitoring of urban areas as a promising field of investigation taking advantage of EnMAP's spatial coverage and revisit capability.

However, owing to the limitations of EnMAPs spatial resolution for urban applications, research should also focus on hyperspectral resolution enhancement to enable retrieving material information on sub-pixel level.

Keywords: urban areas; surface material; EnMAP; imaging spectroscopy; hyperspectral; spectral unmixing; urban application

1. Introduction

For the first time in history, more people are currently living in cities than in rural areas [1]. Because urban areas are the living space of so many people, the current status and development of cities are important topics in various fields of research. Remote sensing can contribute substantially to the characterization and monitoring of cities by providing spatial information. It has many advantages over conventional mapping approaches, of which the continuous area-wide coverage is one of the most important. In addition, the potential of global data acquisitions is an integral feature of spaceborne remote sensing platforms, which allows for global comparisons and analyses. Another advantage is the application of automated mapping methods. These methods enable the retrieval of cost-efficient information of large geographic areas and avoid biases inherently introduced by manual interpretation of aerial photographs or remote sensing imagery by different individuals. Automated approaches facilitate the quantitative comparison of results of different regions and periods (e.g., annual, seasonal), making remote sensing a valuable tool for urban analysis and monitoring.

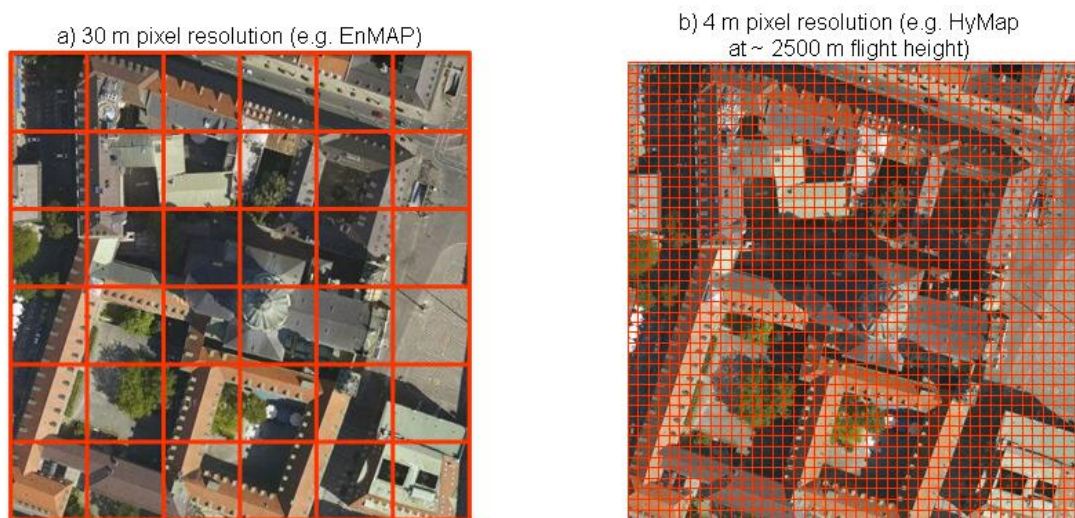
At present, a large range of sensors is available for urban remote sensing. They differ in spatial and spectral resolution, spatial coverage, temporal revisit capability and data costs. The specific characteristics of the different sensors enable the mapping of numerous parameters relevant for various urban applications [2]. Imaging spectroscopy started to be used for urban studies in the 1990s and has subsequently led to detailed and automated urban surface material mapping methodologies. This is possible because of the high spectral information content of imaging spectroscopy data, which enables the extraction of material-specific spectral characteristics. Large potential of imaging spectroscopy systems could be identified combining airborne spectral measurements with laboratory and field measurements [3–5].

However, the potential benefits of spaceborne imaging spectrometers for urban studies have not yet been fully explored. Few urban studies have used spaceborne imaging spectroscopy, as the number of sensors is limited [6–8]. The only spaceborne imaging spectrometer covering the full reflective wavelength range is NASA's Hyperion on EO-1 satellite [9]. ESA's CHRIS (Compact High Resolution Imaging Spectrometer) sensor on the PROBA satellite [10] records only in 19 spectral bands in the visible and near-infrared wavelength range of the electromagnetic spectrum. Additionally, compared to the newest multispectral sensor systems with pixel sizes of less than 10 m (e.g., WorldView, GeoEye), spaceborne imaging spectrometers show a significantly lower spatial resolution that is not sufficient to resolve most of the small-scale urban objects, such as buildings and streets. The average size of urban objects is 10–20 m [11,12], making the use of sensors with a high spatial resolution the logical choice

for urban analysis. On the other hand, there is a large quantity of urban studies using the medium spatial resolution of Landsat data (15 m panchromatic and 30 m multispectral) mostly in the context of urban sprawl analysis (e.g., [13–16]).

These studies indicate the potential of using medium resolution (MR) remote sensing data for addressing urban issues. Imaging spectroscopy data can provide additional information about the surface materials, which is important for a wide range of research questions related to ecological and climatological and human living conditions in cities [17–23]. As a result of the discrepancy between the spatial resolution of spaceborne imaging spectroscopy systems and the average size of urban objects, the majority of pixels contains spectral information of more than one surface material. This is shown in Figure 1(a), where, depending on the size of the urban objects, commonly more than three surface materials contribute to the spectral mixture of a simulated EnMAP Hyperspectral Imager (HSI) pixel. Techniques dealing with the mixed pixel problem of urban areas in airborne hyperspectral data can be found in the study of [24] among others. However, authors assume that for most of the pixels of around 4 m, a maximum number of two spectrally significant materials contribute to the pixel (Figure 1(b)). The mixed pixel problem is getting more complex when using MR spaceborne instruments, where more than two materials contribute to a pixel. Since not many hyperspectral image analysis techniques have been tested and adapted for MR data yet, corresponding sensors and data have not been the first choice for the analysis of complex urban areas.

Figure 1. Spectral mixed pixels: simulated 30 m pixel resolution like planned for EnMAP HSI sensor (a) and 4 m pixel resolution in comparison (b).



This is likely to change with the development of several missions that will provide data of new spaceborne imaging spectrometers on an operational basis. These initiatives include the HISUI mission (Hyperspectral Imager SUite) [25], the HypIRI mission (Hyperspectral Infrared Imager) [26] and the EnMAP mission (Environmental Mapping and Analysis Program) [27]. The technical parameters of these missions are listed in Table 1. The upcoming EnMAP mission will operate a new space borne imaging spectrometer (HSI—Hyperspectral Imager) with a high signal-to-noise ratio. The expected high data quality and its extensive spatial coverage of 900 km² per scene open up possibilities for the

upscaling of existing imaging spectroscopy approaches developed for airborne data with limited spatial coverage. However, a direct transfer of these methods to spaceborne imaging spectroscopy data will be challenging because of the difference in spatial resolution between the airborne and EnMAP HSI data. New or adapted methods will be required to exploit the full information content of the EnMAP HSI data for urban analysis.

The objective of this paper is to compile and highlight relevant fields of application and promising future methodical developments that may contribute to explore the potential of the EnMAP mission for urban studies. For this purpose, an extensive literature review was undertaken to identify the main fields of urban applications and the required parameters that can be derived from remote sensing imagery. Furthermore, a survey of state-of-the-art hyperspectral and multispectral image processing techniques has been carried out. As a synthesis, we outline the future research directions necessary to optimize EnMAP HSI data for urban analysis in the identified application fields.

Table 1. Technical parameters of upcoming spaceborne hyperspectral missions [28,29].

Mission	HISUI		HypIRI		EnMAP
	<i>Hyperspectral</i>	<i>Multispectral</i>	<i>Hyperspectral</i>	<i>TIR</i>	<i>Hyperspectral</i>
Sensortype					
Country and Organisation	Japan METI		USA JPL/NASA		Germany GFZ/DLR
Spectral range (nm)	400–2,500	450–900	400–2,500	4,000–12,000	420–2,450
GSD (m)	30	5	60	60	30
Swath at nadir (km)	30	90	145	600	30
Spectral resolution (~ nm @ FWHM)	10 VNIR, 12.5 SWIR	TBA	10 VNIR 80 SWIR	400 TIR	6 VNIR, 10 SWIR
Number of bands	185	4	>200	8	232

2. The Hyperspectral EnMAP Mission

The EnMAP mission is a German hyperspectral satellite mission that will provide high quality hyperspectral image data with a frequent revisit capability [30]. The mission is predominantly a scientific program addressing a research-oriented user community [31,32]. The major objectives of the mission are to measure, derive, and analyze diagnostic parameters which describe vital processes on the Earth's surface. Those biospheric and geospheric processes are assimilated in physically-based ecosystem models and ultimately provide information reflecting the status and evolution of various terrestrial ecosystems. Based on these quantitative measurements, remote sensing products can be generated which could only be produced in the frame of scientific airborne hyperspectral campaigns so far. The launch of the EnMAP satellite is scheduled for 2015.

The satellite will be operated on a sun-synchronous orbit at 643 km to observe any location on the Earth's surface under defined illumination conditions. In order to achieve short revisit times of up to 4 days, a high performance three axis control allows pointing of the hyperspectral sensor up to $\pm 30^\circ$ in across track direction, such that an area of interest can be observed from several orbital paths. This increases the probability of achieving cloud-free data takes. The global revisit capability

under a quasi-nadir observation ($\pm 5^\circ$) is up to 21 days in the equator region. Although this enables the observation of areas of interest all over the world, it is not a primary objective of the mission to acquire a complete global coverage. Table 2 lists the EnMAP HSI instrument parameters. The spectral configuration in combination with a high radiometric resolution and stability will allow for the measurement of subtle reflectance changes related to biospheric and geospheric processes of the Earth's surface.

Table 2. EnMAP HSI Instrument parameters [33].

Instrument type	Hyperspectral Imager (HSI) with two prism imaging spectrometers, split FOV between VNIR and SWIR	
Scanning method	Push-broom, pointing capability up to $\pm 30^\circ$ off nadir across track	
Swath width (nadir)	30 km	
Ground sampling distance	30 \times 30 m at nadir at $\pm 48^\circ$ northern latitude	
Radiometric resolution	14 bits/pixel	
Spectral ranges (no. of bands)	VNIR 420–1,000 nm (96)	SWIR 900–2,450 nm (136)
Spectral resolution	8.1 \pm 1.0 nm	12.5 \pm 1.5 nm
Spectral sampling distance	6 nm	10 nm

In the frame of the EnMAP mission pre-launch science activities, a toolbox has been developed at the Humboldt-Universität, Berlin, Germany. The EnMAP-Box [34] is a license-free and platform-independent software package that enables the exchange, evaluation, and distribution of algorithms (evolving toolbox) for the analysis of hyperspectral remote sensing data. The focus is on EnMAP-specific processing algorithms. Currently, the EnMAP-Box contains only few algorithms. Therefore, this paper can serve as a starting point to highlight potential techniques and algorithms that are relevant for analyses in the urban context and give recommendations for future developments that potentially can be of value and can be integrated into the EnMAP-Box.

3. Application Fields of Urban Remote Sensing

Urban remote sensing studies are carried out for a large variety of applications. For this paper we reviewed 146 publications on remote sensing of urban areas. From this review, four application fields are commonly mentioned as the objective or background in those studies and include: urban development and planning (28%), urban growth assessment (16%), risk and vulnerability assessment (9%) and urban climate (16%). The other 31% focus mainly on methodical improvements especially for urban analysis, such as land cover mapping or spectral analysis techniques. It has to be noted that it is not always possible to clearly separate between the specified four application fields, since some parameters are relevant for several applications. Environmental and climatic parameters are also important in the frame of urban development and planning, for example. However, since they are seldom incorporated in the urban planning praxis [35], they remain predominantly the domain of scientists. Therefore, we address urban climate as a separate application field in Section 3.4.

Table 3 gives an overview of the four application fields and relevant parameters. Urban land cover is a common parameter which is relevant for all application fields and serves as a basis for the further derivation of value added information. The parameters in Table 3 are sorted according to scale and sensor type. The sensor types are grouped into medium spatial resolution (MR) data with a pixel size of >20 m (e.g., Landsat TM/ETM) on the one hand, and high and very high spatial resolution (HR) imagery with a pixel size of <20 m (e.g., SPOT) and <5 m (e.g., IKONOS, Quickbird) on the other hand, both multispectral data. In addition to satellite-based sensors, airborne multispectral sensors providing cm-resolution are frequently used to analyze urban environments [36–38]. However, these sensors are mostly not radiometrically calibrated so that the corresponding techniques will not be considered in further detail in this paper. In addition to multispectral data, also hyperspectral data is applied. For this data, HR data includes pixel sizes of 2–20 m (airborne hyperspectral sensors) and MR data includes pixel sizes of >20 m. It should be noted that in the category of MR hyperspectral data only three journal articles have been published, all using Hyperion [6–8] (according to Web of Knowledge, 2011-2-9). The requirements of the application field in combination with the selected sensor provides the framework for the selected image processing methods that are used to derive the desired information [39].

Table 3. Dominant application fields and relevant parameters with respect to the different scales and sensor types

Application field	Multispectral remote sensing		Hyperspectral remote sensing	
	MR	HR	MR	HR
Urban development and planning	Regional mapping of build up area [40], imperviousness [41], vegetation density [42], landscape metrics [43–45]	Building and vegetation structure [12,46], biotope mapping [47]	Urban land cover materials [7,8], imperviousness [6]	Local mapping of build up area, imperviousness, vegetation density [48], material mapping [4,24], urban structure mapping, biotope mapping [49]
Urban growth assessment	Built up area, land cover change [50–53]	Change detection at building level [54]		Change detection at building/material level [55]
Risk and vulnerability assessment	Large scale physical parameters—see other application fields	Mapping physical parameters for vulnerability estimation e.g., transportation network, open spaces [56,57]		Identification of hazardous materials [58,59]

Table 3. *Cont.*

Urban climate	Vegetation density e.g., by NDVI [60], heat island, related parameters: imperviousness, vegetation, albedo [61,62]	Building and vegetation structure [46]		material-based land cover, building and vegetation structure [17,63]
---------------	--	--	--	--

3.1. Urban Development and Planning

In Europe, many governments define objectives regarding the land use, urban structure or amount of impervious surface (buildings, streets, *etc.*) that are desired for a sustainable city. Imperviousness is a key parameter for urban analysis [20] and urban planning at different spatial scales. For example, at regional scale it is used as an indicator for the spatial extend of urban areas [50] or as an indicator of the negative effects of ongoing consumption of land resources [41]. At local scale, this parameter is especially of interest for urban planners aiming to reduce the percentage of impervious surfaces to avoid negative climatic effects, such as overheating (e.g., [64]). A further issue is the reduction of surface water runoff by unsealing the urban surface [65,66] or by using partially pervious surface materials. To evaluate these local scale effects, precise mapping and monitoring of the surface cover and their characteristics (e.g., regarding the ability of runoff water to infiltrate the surface) are needed.

Urban structure is another important parameter in the application field of sustainable urban development and can be described by location, orientation and density of the different urban objects such as buildings or vegetation. The analysis of urban structure provides insights into the configuration of a city and can be an indicator for social, economical or environmental aspects [66,67]. For example, type, location and density of vegetation within a neighborhood influence the living quality, because green neighborhoods are generally more appreciated by citizens. Different approaches to derive structure parameters from remote sensing data can be found in literature, for example by applying texture analysis [68] or spatial metrics [60]. For this purpose, HR data are typically employed to characterize urban structure owing to the small size of urban objects. Herold *et al.* [68] characterized textural features of urban structures on the level of building blocks by applying a combination of landscape metrics and gray-level co-occurrence matrices. Textural measures and neural networks have also proven highly suitable for urban land-use/land-cover classification [69,70]. Analyzing urban structure with MR data allows for comparisons of cities, because complete spatial coverage of the cities is possible with this type of data. Huang *et al.* [43] calculated spatial metrics based on a land cover classification of Landsat data for 77 cities in various parts of the world. The aim of this study was to analyze urban form and describe the differences among world regions, developed and developing countries. Several socio-economic development indicators were evaluated to gain more insight in the differences. The results of the study clearly show that urban agglomerations of the developing world are more compact than those in Europe or North America. In combination with additional information, such as census data, the socio-economic characteristics related to different urban structures can be studied in detail [71].

For sustainable urban development, urban ecology plays an important role. Urban ecology focuses mainly on the urban vegetation, which influences the quality of life of citizens and provides a living space for animals and plant species. Therefore, studies have been carried out mapping urban vegetation density and structure (e.g., [11,60]). Vegetation density within an urban area can be mapped at a regional scale. However, a higher spatial resolution is preferable for mapping urban vegetation, because urban green consists often of small objects (e.g., a lane of trees along a road or a small neighborhood lawn). These small occurrences of vegetation in urban environments can still be of significant importance for climate, urban animal habitats, and general appreciation of the area. Next to the mapping of vegetation structures, urban biotope mapping is a demanding task in European cities. For example, Bochow *et al.* [55] performed a classification of urban biotope types using airborne hyperspectral data. Subsequently, they compared the resulting maps with governmental data to identify locations that have changed. Using this approach, future field surveys required for updating governmental biotope maps can be limited to those locations that have changed, thus reducing costs and resources.

3.2. Urban Growth Assessment

Urban areas often grow very fast, especially in developing countries. For planners and scientists, the growth of the city, the changes in building density, and the decrease of vegetation density provide useful indicators to characterize the dynamics of urban developments. Monitoring of informal urban growth is important for governments to enable them to supply appropriate infrastructure (roads, schools, *etc.*). Spaceborne remote sensing is very much suited for this particular application, where time series of maps can be generated over many years as frequent coverage and largely automated analysis of the data is possible.

One of the most important parameters for urban growth assessment is the monitoring of built-up areas. Developing countries often lack detailed building maps, whereas western countries have to update detailed cadastral maps regularly. Therefore, remote sensing images are used at different spatial scales to derive information about built-up areas, whereas for mapping single buildings, high resolution remote sensing data is used in most studies. By developing and applying object-based classification approaches [72] or using texture information [73–75], buildings of different sizes can be detected up to parcel level. Durieux *et al.* and Banzhaf *et al.* [52,54] use an object-based approach to identify built-up areas in SPOT data to analyze urban sprawl. When MR data is used, the corresponding analyses mainly aim at the mapping of built-up areas with different densities [76], rather than the detection of single buildings. At regional, national or global scale, the main focus is to monitor land cover changes in the transition zone covering urban, peri-urban and rural areas [40]. Examples include the global urban maps derived from MODIS (Moderate Resolution Imaging Spectroradiometer) or the Nighttime lights products [45].

General land cover maps or maps of imperviousness are also used for urban growth assessment (e.g., [77]). After deriving a map of the urban extend for different time steps (commonly between one and ten years, depending on available data), differences between maps are calculated. For example Madhavan *et al.* [50] carry out such a post-classification comparison of vegetation-imperviousness-soil (V-I-S) maps to analyze the growth patterns of Bangkok using Landsat TM data. Weng *et al.* [78] use ASTER (Advanced Spaceborne Thermal Emission and Reflection Radiometer) data to map impervious

surface of Indianapolis (USA) in 2000, 2001 and 2004 as a key indicator for urbanization. When multiple scenes within one year are available, this can be used to analyze spectral differences over time between the various land cover types to identify urban eco-regions, as implemented by Schneider *et al.* [45]. They used low resolution MODIS data (500 m pixel size) to create a map of urban extend at global scale.

Other studies have focused on the analysis and comparison of the structural development of cities. As with all monitoring tasks, multi-temporal data is required. Medium and low spatial resolution remote sensing data is frequently used for urban growth analysis because of their frequent and extensive spatial coverage. Taubenböck *et al.* [22] analyzed Landsat TM, Landsat ETM and TerraSAR-X images recorded since 1970 to measure and characterize the past effects of urban growth. This way, spatial characteristics of urbanization dynamics are shown, allowing indirect conclusions on causes for the future trend of urbanization. Hybrid approaches, such as using historical maps for time steps before remote sensing data became available, provide a means to generate longer time series [79]. A subsequent analysis of the mapped urban sprawl combined with population numbers [80] can support urban growth modeling. This can provide important insights required for the prediction of needs for housing and infrastructure.

3.3. Risk and Vulnerability Assessment

With increasing urban population, settlement into and industrialization of highly exposed regions, the number of people potentially affected by hazards occurring in urban areas increase substantially. This makes it even more important to provide sufficient information to assess the risk of different hazards and to assess the vulnerability of the area to damages or disasters. Physical parameters that are required to increase the knowledge about risk and vulnerability can be provided by remote sensing [56,57,81], providing governments with important information before a disaster happens. Examples are building density, building types or accessibility (e.g., information on the road network) and land use/land cover information. To evaluate the risk of various types of hazards, of course different information is relevant. Taubenböck *et al.* [56] provided a concept to assess vulnerability and risk with remote sensing for which land cover, building density and population distribution are important parameters. Bhaskaran *et al.* [82] used airborne hyperspectral data to identify buildings that are vulnerable to hail storms as part of a post-disaster support system. Dousset *et al.* [57] monitored the heat wave in Paris in August 2003 for applications to environmental risk assessment and to health alert systems. Here, AVHRR (Advanced Very High Resolution Radiometer) satellite images were processed to retrieve the diurnal variations of surface temperature with a land cover classification mapped from the multispectral SPOT-HRV sensor.

After a disaster occurs, urban remote sensing can support mapping of the damage [83], for example the damage assessments after the earthquake in Haiti in January 2010 [84] or the contributions to risk assessment following the Earthquake in West Sumatra and the Mentawai Tsunami 2010 [85]. Frequent temporal coverage is advantageous for this application, because it enables a comparison of the situation before and after a disaster. This can also provide public authorities (civil protection and civil security) and non-governmental organizations, such as the German Federal Agency for Technical Relief (THW), the European Monitoring and Information Centre (MIC) or the United Nations (UN), with detailed information on a particular disaster in a short period of time.

Hyperspectral data can also be used to detect hazardous materials, such as asbestos [58,59]. Marino *et al.* [86] analyzed the interactions between natural risks, industrial installations, agricultural areas, water resources and urban settlements. This was accomplished using the airborne MIVIS sensor to produce a land use classification that was combined with additional information such as lithology and geological structure.

3.4. Urban Climate

The differences between rural and urban areas at medium scale are one of the main research topics for urban climate analysis. The urban heat island is the most well-known effect in this context. It describes the phenomenon of higher air and surface temperature in urban areas compared to the surrounding rural areas [87]. This phenomenon is mainly studied at regional scale, covering the whole city and its surroundings. For this purpose, MR remote sensing data such as Landsat (TM/ETM+) is best suited. Often thermal remote sensing (wavelengths between 4 and 14 μm), such as Landsat TM/ETM+ thermal band or ASTER, is used to determine the surface urban heat island, but it does not provide information on air temperature. Since EnMAP will not have a thermal band, approaches aiming to describe surface temperature by related spatial characteristics are of larger interest for this study. Such approaches include the mapping of the Normalized Difference Vegetation Index (NDVI) [88] or spatial indices such as imperviousness after having established a correlation with land surface temperature [61,89]. Yuan *et al.* [62] found that imperviousness can serve as a complementary metric to NDVI for monitoring of the urban heat island effect. Such relationships were also found for vegetation cover derived by spectral unmixing [90,91] or albedo [92].

Micro climate is studied on a local scale, requiring HR remote sensing data. In addition to the location and orientation of the different urban objects, urban surface materials have significant influence on the urban micro climate [93]. Among others, Xu *et al.* and Jung *et al.* [63,94] focus on urban micro climate, by combining thermal airborne remote sensing data with hyperspectral data for land cover mapping. Heldens *et al.* [95] used a detailed surface material map derived from airborne hyperspectral data as input for a micro climate model with which information on temperature, humidity, wind speed, *etc.* can be derived. Other studies have mapped surface albedo [96,97] or urban form and materials [93] to support the modeling of urban energy fluxes.

4. Image Analysis Approaches

An assessment of the potential of the EnMAP mission for urban analysis requires an evaluation of methodologies that are currently available for the information extraction from earth observation data. This section provides such evaluation. It forms the basis for the discussion in Section 5 on how these approaches might be adapted for use with EnMAP HSI data. In most cases land cover classification algorithms are the starting point for the derivation of value-added urban remote sensing products. Spatial inventories of the urban land cover require an appropriate classification scheme, which provides the user with an overview on the urban area at different levels of thematic detail. This section begins with an introduction to common classification schemes (Section 4.1). Next, it provides an overview of the main

trends of multispectral image processing techniques for urban analysis followed by a description of common approaches and strategies using hyperspectral data.

4.1. Classification Schemes

Selection of an appropriate classification scheme is very important and depends on the available data and information requirements [98]. Further, spatial mapping of the urban surface requires ideally a classification scheme that is universally valid, and thus, applicable for various thematic applications, ranging from mapping of building structure to imperviousness assessment in the urban fringe [77]. The majority of classification schemes are structured in a hierarchical way [99]. The hierarchical land use/land cover classification scheme of Anderson *et al.* [100] has been adopted by many subsequent studies. This was originally developed for the US Geological Survey (USGS), with broad land cover classes (urban, forest, water, *etc.*) at the first level, which are differentiated at a second level into urban land use classes such as industrial or residential. At a third level, these classes are further distinguished, e.g., into different densities. This classification scheme serves as a basis for the development of other systems, which are adapted to the specific applications and detail of land cover inventories (e.g., [4,5,24]).

Another frequently used classification scheme is the V-I-S concept developed by Ridd [101]. This concept is often used for analysis at medium spatial resolution (e.g., [20,102]), comparable with the scale of Andersons Level I. According to this concept, urban area can be modeled by vegetation, impervious surface and soil due to the assumption that they have different spectral characteristics. It is assumed that these three classes sufficiently describe urban areas for most urban studies.

4.2. Multispectral Approaches

There are numerous methods and strategies available for image classification. Lu *et al.* [39] provide an overview of the various classification approaches. Pixel-based approaches are most common. Traditional parametric classifiers, such as maximum-likelihood are regularly applied for urban land cover classifications (e.g., [50,103]). Sub-pixel mapping in the form of linear spectral unmixing is widely used as urban objects are relatively small [104]. This issue is discussed in more detail in the next section (Section 4.3). Linear spectral mixture analysis is also commonly used to map urban areas according to the V-I-S concept (see Section 4.1), where vegetation, impervious surface and soil, which commonly occur within meters of each other, are considered as three endmembers in an unmixing model [105–107]. However, these endmembers may comprise several surface materials that cannot be differentiated due to limited spectral information available from multispectral sensors. To improve the quality of the endmembers, in several studies the impervious class is replaced by high and low albedo endmembers (e.g., [20,102,108]). The disadvantage of this approach is that the low albedo endmember may also substitute for water and shadow. Each of the studies mentioned above remark that there is a difficulty in discriminating impervious surfaces from soil using spaceborne multispectral data. Thus, using hyperspectral data or reference endmembers in addition to image endmembers could improve the identification and discrimination of impervious surface [6].

Since traditional parametric classifiers (also named as statistical approaches) assume a normal distribution of the data, which is usually not the case, non-parametric classifiers are a common topic of research [39]. Due to the complexity of urban landscapes, which often does not fit to the requirements of parametric approaches, an increasing number of land cover classifications is carried out using techniques such as decision trees (e.g., [109]) or neural networks (e.g., [110,111]), where neural network techniques can also be applied to derive sub-pixel land cover maps (e.g., [65,112]). Another example is the use of support vector machines (SVM). For example, Esch *et al.* [41] employed a SVM classifier which is trained using high resolution imperviousness maps and cadastre data of one city. Subsequently, the SVM was used to estimate imperviousness of Landsat ETM+ data of the whole state of Bavaria, Germany.

Classification techniques are not only applied to single pixels but often also to clusters of pixels (objects, fields, segments), for example resulting from image segmentation. Object-based image analysis is mainly applied with HR imagery [72,113,114], since such data allows for the accurate detection of the distinct borders of urban objects by segmentation algorithms.

Along with classification techniques, other image processing methods are commonly applied to analyze urban areas using multispectral remote sensing data and include indices and texture analysis. For example Zha *et al.* [40] derived a built up index for Landsat data, similar to vegetation indices such as NDVI. The Normalized Difference Built up Index (NDBI) is defined as $(TM5-TM4) / (TM5+TM4)$, making use of the 4th and 5th Landsat TM band located in the near infrared ($0.77 \mu\text{m}$ – $0.90 \mu\text{m}$) and short wave infrared ($1.55 \mu\text{m}$ – $1.75 \mu\text{m}$) range of the electromagnetic spectrum, respectively. Texture measures analyze the spatial patterns within a remote sensing image and can be used to map urban extent [73] or analyze urban structure via spatial metrics (e.g., [12,43,60]). For texture analysis HR data is commonly used, because detailed spatial patterns are of greater importance than spectral information.

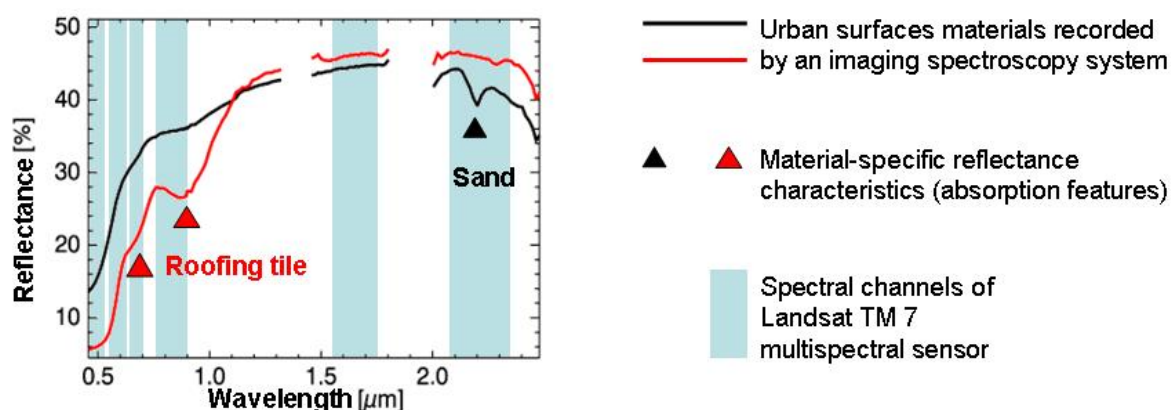
4.3. Hyperspectral Approaches

For hyperspectral image processing knowledge about spectral characteristics of the materials is necessary and forms the basis for the identification of urban surface materials. Each surface material has a specific spectral signature that is determined by its physical properties and chemical composition (Figure 2). Imaging spectrometers are especially suitable for material identification as they measure the solar reflectance in many narrow and spectrally contiguous bands. Figure 2 shows that as a result, almost continuous spectral signatures can be retrieved for each pixel, thus resolving the narrow material-specific reflectance characteristics. On the other hand, multispectral systems contain only limited compositional information [115] recorded in broad spectral bands (marked in blue in Figure 2) that are not contiguous. Thus, hyperspectral sensors are better suited to measure specific physical properties of surface materials, which in turn, can be used to discriminate and identify these surface materials [116].

In addition to the physical and chemical properties of a surface material, there are several other factors that may influence the spectra of urban surface materials (e.g., [4,59]). For example, the effects of aging are an important research topic. Usage, dust, and erosion can largely change the physical and chemical spectral properties of a material, and thus its spectral signature (e.g., asphalt as described by Herold and Roberts [117]). Additionally, the Sun illumination angle, the orientation of the urban objects, and the viewing geometry of the sensor can have significant effects on the spectral signature. This is described by the bidirectional reflectance distribution function (BRDF) [118–120]. Another major factor

is shadow, which reduces the albedo of the surface material and thus, can hide the spectral reflectance characteristics making the detection of the material challenging. Therefore, surface material mapping approaches usually include shadowed areas as their own class for a more reliable quantitative assessment of surface material abundances. Bochow *et al.* [121] developed a robust method to detect shadow. The image is multiplied with the diffuse radiance part in order to model the brightest shadow pixel in that image. It follows a step-by-step process of masking out dark surfaces such as asphalt and water to avoid misclassification. An algorithm to reconstruct reflectance spectra from shadowed areas was developed by Richter and Müller [122]. The algorithm corrects spectra for shadows cast by clouds and buildings based on the detection of core shadow and expanded shadow regions to reduce shadow-pixel misclassification. This is accomplished using a shadow function, which uses information acquired from one spectral band in the visible and one or more spectral bands in the near infrared region.

Figure 2. Spectral signatures of typical urban surface materials with its material-specific reflectance characteristics; multispectral systems, such as the Landsat TM 7 sensor, are not able to record the narrow spectral characteristics due to the broad spectral bands.



Knowledge of the spectral characteristics of urban surface materials and the characteristics of the additional factors mentioned above are crucial for applying spectral analysis techniques to produce accurate maps of urban areas using hyperspectral data [4,59]. Traditional parametric classification approaches are often applied to multispectral data (e.g., [50], see also Section 4.2) to map urban land cover. These approaches, such as maximum-likelihood classification, are sometimes also applied to hyperspectral data, either on the original reflectance bands or on transformed spectral bands (e.g., [5,123]). However, because of the Hughes phenomenon [124], the classification performance of traditional statistical classification approaches levels off after a certain number of bands and then even decreases, which makes such approaches less suitable for hyperspectral data analysis. Therefore, transformations are commonly applied to reduce data dimensionality, for example using a minimum noise fraction transformation (MNFT) or a principal component transformation (PCT). However, this transformation changes the spectral characteristics of the image data, and thus, cannot be directly related to the physical properties or composition of the surface material.

In order to use the full information content of the hyperspectral image, feature based classification technology and spectral matching techniques have been developed. Heiden *et al.* [4] numerically

describe the spectral reflectance curve using various feature functions, such as mean, standard deviation and ratios of the reflectance between two wavelengths, by the area under the feature in the spectrum, and by the absorption depth and position. Spectral matching techniques assess the similarity of an image spectrum to a known class spectrum [125,126]. Examples of similarity measures are spectral information divergence (SID) [127], Euclidean distance (ED) or spectral angle mapper (SAM) [128]. SAM was applied to identify various urban materials [82,129]. The spectral feature fitting technique (SFF) [130] is very common as well and has for example been applied for the detection of asbestos-cement roofing sheets [59]. It is also a core technique in the USGS Tetracorder and Expert System [131]. For the successful application of such techniques high quality radiometric and atmospheric correction are of utmost importance to enable comparison between spectra of different images and spectral libraries.

In addition to statistic and quantitative classification methods, non-parametric classification techniques are frequently applied on hyperspectral data. Artificial neural networks (ANN) [132] are becoming more popular, as well as SVM [133–135] because these techniques are able to cope with complex classes and the high dimensionality of hyperspectral data.

However, these approaches only assign one material class to a pixel. This is not realistic for urban areas as already shown in Figure 1. To deal with the mixed pixel problem described in Section 1, linear spectral mixture analysis (LSMA) [136] has been introduced. The recorded reflectance of a mixed pixel is calculated as the integrated sum of reflectances of all types of surfaces within the instantaneous field of view (IFOV) of the sensor weighted by their area coverage. This technique allows the estimation of the abundance of each surface material (endmember) that contributes to the spectral mixture of a mixed pixel. LSMA was applied by [3,137,138] to map urban land cover at a detailed level. The accuracy of the results of such studies strongly depends on the precise selection of endmembers (EM) and meaningful results can only be achieved if the EM are spectrally distinct. However, Somers *et al.* [139] concluded that most LSMA cannot account for the temporal, spatial and within-class variability of EM. Therefore, Rogge *et al.* [140] integrate spatial-spectral information into a fully automated EM extraction tool and have proven to detect EM in the context of geological applications. Although images of urban areas comprise a high number of spectrally distinct endmembers [4], they are additionally characterized by a large within-class variability [4,118] as the result of aging, BRDF effects, and shadow as described above. In order to deal with the per pixel EM variability, the Multiple Endmember Spectral Mixture Analysis (MESMA) was developed to allow the types and number of EM to vary for each pixel [141]. Some unmixing approaches assume the contribution of different materials to the image spectrum to be non-linear, which in many cases is more realistic, especially in urban areas where scattering of neighboring objects occurs frequently [142]. However, because of the complexity of such models they are seldom applied. A comprehensive overview of spectral unmixing algorithms and a discussion about linear versus non-linear mixing spaces throughout various applications can be found in [143,144].

Mathematical approaches, such as morphological profiles, have been developed to analyze urban hyperspectral data [145,146]. In these approaches, spatial organization is explicitly taken into account. Plaza *et al.* [135] provide an overview of several techniques to combine spatial and spectral information, including morphological profiles and Markov Random Fields. Spatial information (e.g., neighboring pixels) can provide very useful a priori information for the classification of urban areas. However, high

spatial resolutions are generally required for this, because then the borders of urban objects can easily be detected. As noted previously in Section 4.2, object-based approaches are promising and are often applied on high spatial resolution data. Also for airborne hyperspectral data, the number of studies using such techniques is increasing. An interesting example is the use of SVM to model and classify a segmented image [133,147].

5. Discussion of the Potential of EnMAP for Urban Studies

This section discusses the future research directions necessary to optimize EnMAP HSI data for urban analysis. First, we outline several promising methodological issues, for example a systematic analysis of the spectral information content of an EnMAP HSI pixel in the urban context and the development of suitable training databases to enable advanced land cover mapping with spectral mixture analyses. Second, a detailed material oriented land cover map should improve higher level products, such as urban indicators relevant for urban planning. Third, if the urban land cover mapping and derived indicators are of high quality, they can be used for an advanced and frequent monitoring of urban areas, which is of high interest for the application-oriented user community. Finally, we think that data fusion gains in importance for many urban applications focusing for example on structural information of a city and climatic issues.

The main strength of the EnMAP HSI is its high spectral resolution, which enables a quantitative, material-oriented identification of urban land cover classes. An improvement of urban land cover classifications, using the hyperspectral HYPERION sensor in comparison with multispectral sensors, could be confirmed by early studies of [7,8]. Since urban land cover mapping is the basis for many applications and especially for those described in Section 3, a wide range of future studies are likely to focus on the development of strategies for a material-oriented land cover mapping.

However, the sensitivity of the EnMAP HSI data for material mapping has yet to be investigated. In the urban context, sub-pixel analyses are necessary to cope with the small objects and high heterogeneity of the landscape [8,42,105]. This requires a systematic analysis of the spectral information content of an EnMAP HSI pixel in the urban context. For this purpose, the minimum fractional abundance of a material that has to be present in a pixel to be detectable by the HSI has to be evaluated. Further, HSI characteristics, such as the spectrometer's sampling interval, spectral resolution, signal-to-noise ratio (illumination and reflectance dependent), the point spread function (PSF), and a material's surface properties all influence whether the HSI can detect key spectral features that are characteristic for the given material [148,149]. Techniques such as the band detection limit (BDL) and the material detection limit (MDL) might be used to quantitatively evaluate these factors [150].

When making use of techniques such as spectral mixture analysis, the abundances of certain surface materials within a pixel are estimated, and thus providing valuable quantitative information in addition to the qualitative information (land cover classes). This is interesting not only for advanced land cover classifications, such as required for urban development and planning, but also for risk assessment. An example is the identification of hazardous materials (e.g., asbestos) during an emergency [58]. However, the definition of pure pixels for training or endmember data sets in the urban context will be challenging due to the spatial resolution of EnMAP HSI. Therefore, the use and integration of external spectral image libraries as prior knowledge for sub-pixel analyses will be promising. This is a continuing field

of research, as results have only been shown for specific study areas using local spectral libraries so far. With regard to the global acquisition capability of EnMAP HSI data, individual libraries may not be applicable to all areas of interest.

According to the spectral resolution of EnMAP HSI data, we assume that it is worth to investigate the use of predefined mixed spectra within those spectral libraries. Urban areas can be classified by structural types, such as industrial sites, parks, cemeteries and row house development as an example of the various residential structural types [151]. Each structural type is composed of a characteristic combination of urban surface materials. As a German example, impervious surfaces of industrial sites are predominantly covered by concrete. Roofs of the large buildings are covered typically with metal and hydrocarbon materials. In contrast, row house development are characterized by buildings that are mostly covered with red roofing tiles with large green areas in between [152]. These typical combinations of urban surface materials can produce specific spectral mixtures in an EnMAP scene with a spatial resolution of 30 m. Although those mixtures differ regionally and globally [153], the use of a mixture instead of pure material spectra can be an alternative approach for a more detailed analysis of urban areas with EnMAP HSI data.

Spectral libraries can also be used for classification purposes by comparing the image pixel spectra with a library spectrum, using spectral comparison measures [127]. This has been realized for example with the Tetracorder system [131] and could be also a possible option for identifying typical urban surface material mixtures as discussed above. Such an approach requires that the mixed spectra can be recognized by specific spectral reflectance characteristics such as absorption features. Another promising approach applying spectral comparison measures was presented by [154], evaluating the significance of spectral comparison values according to the mixture information.

In order to retrieve reliable results from the above described methodologies, especially when carrying out multitemporal analyses, BRDF effects have to be considered. The frequent availability of EnMAP HSI data will be ensured by the pointing capability of the EnMAP satellite. As a result, time series images are recorded under different viewing conditions. This requires additional research to separate changes in pixel spectral signatures as a result of the different viewing angles from real land use changes. In this context, the BRDF of the various urban surfaces has to be taken into account during image analysis. These effects have been studied for natural surfaces, for example with the spaceborne hyperspectral sensor CHRIS/PROBA [155,156]. Temporal effects are considered within the BRDF in order to model and quantify BRDF canopy patterns as they relate to in situ biophysical measurements and phenological changes [157]. The BRDF of urban surfaces was intensively investigated by [158,159] and a large-scale bidirectional reflectance model for urban areas was developed by [120] for pixel sizes of more than 500 m × 500 m. Such models have to be adapted to the spatial and spectral requirements of the EnMAP HSI data.

An effective and application oriented use of the material information is the derivation of urban indicators that are often used to support the quantitative characterization and delineation of urban areas, typically at regional scale. Using EnMAP HSI data such indicators can be calculated with a higher accuracy based on a material-based inventory of the urban surface. For example, with current spaceborne multispectral sensors the mapping of the key parameter imperviousness is often limited due to the difficulty in separating impervious surfaces (e.g., concrete) and soil (see also section 4.2). With

EnMAP HSI data, impervious surface mapping can be improved because the within-class variation of impervious surfaces and soil can be taken into account. This expectation was confirmed in a study comparing the use of HYPERION and ALI (Advanced Land Imager) for imperviousness mapping [6]. Thus, new indicators characterizing imperviousness, built-up areas and vegetation on a spectral basis, instead of simply albedo, can be expected to be derived with a higher thematic detail.

Based on the literature review, it can be concluded that a wide range of studies apply MR multispectral data. The monitoring of the development of built-up areas, imperviousness, or vegetation plays an important role, and thus, monitoring can become one of the key applications of EnMAP HSI data in the urban context. The spatial coverage of the HSI and the revisit capability of the EnMAP satellite enable a frequent and cost-effective mapping of large urban areas. For example, for urban planners the EnMAP HSI data could enable the analysis of urban development trends in relation to socio-economic and political factors, and to model and monitor the impacts of planning activities. It can also support studies analyzing the global trend of urbanization [22,45]. Spatio-temporal analysis (e.g., of megacities) helps to better understand urban systems and their dynamics. In order to forecast future spatio-temporal development, it is necessary to identify urban development stages, to learn from processes observed in other cities, and to relate and interpret causes and consequences of planning activities or uncontrolled processes [14]. With regard to the global availability of the EnMAP HSI data, consistent continuous monitoring of dynamically sprawling cities is possible. The material-based inventory of cities using EnMAP HSI data holds the potential for a more thematically detailed analysis of the heterogeneous urban structures. It requires the consideration of new indices for the analysis of urban sprawl dynamics that are able to exploit the full information content of the EnMAP HSI imagery.

Although MR data can be a suitable basis for multitemporal analysis, there are various applications requiring HR data to retrieve structural information about the urban area. For example, a spatially detailed analysis of urban structures in combination with material information is of high interest for urban planners at local scale. Therefore, image data fusion will be a promising technique for future information retrieval from EnMAP HSI data. An overview on image and data fusion is given for example in Zhang [160]. Within the context of EnMAP, iconic data fusion at pixel or signal level is of highest interest. Numerous techniques and methods have been developed on iconic image fusion, where panchromatic images with high spatial resolution are combined with multispectral images of low spatial resolution but with higher spectral resolution [161]. In order to ensure that no spectral distortions occur while increasing the spatial resolution, spectral preserving fusion methods have to be used, for example those developed by Ehlers *et al.*, Ehlers, or Palubinskas *et al.* [162–164]. As described in Section 4.3, spectral mixture analyses allow extracting the abundances of (known) reference spectra in low resolution pixels, but not their localization inside the pixel [165,166]. This could be overcome by employing panchromatic, multispectral images of higher spatial resolution, digital elevation models or SAR (Synthetic Aperture Radar) data. The distinctive shapes of urban objects (e.g., building, road) allow the precise allocation of the materials that can be retrieved from the medium resolution pixels of hyperspectral EnMAP HSI images using sub-pixel analysis. Thus, the material-oriented land cover mapping can be available for planning activities at local scale.

For urban climate studies, data fusion at feature or knowledge level can be an interesting technique to extend the hyperspectral data with thermal information. Urban surface materials and structure directly

influence the urban climate [167]. Therefore, it would be of interest to study these characteristics together with thermal patterns. Such studies have already been carried out at local scale with airborne thermal and hyperspectral data (e.g., [63]). However, it is hardly feasible to study the whole spatial extend of the urban heat island with airborne data because of the limited spatial coverage. Approaches using fusion techniques combining EnMAP HSI data with its larger spatial coverage with data of thermal sensors covering a similar area (e.g., ASTER) can open up new ways for urban climate analysis.

6. Conclusions and Outlook

In this paper we carried out a literature review to identify if the upcoming spaceborne hyperspectral EnMAP mission can contribute to urban applications. Although there is a discrepancy between the average size of urban objects and the spatial resolution of the EnMAP HSI pixels, we conclude that there is potential in exploiting the greater spectral information content for urban analysis. This requires research to resolve the spectral composition of a pixel in respect to the contributing urban objects and it requires the development of new methods and strategies to exploit the full spectral information content of the EnMAP HSI. Further, our literature survey showed a large number of studies making successful use of medium resolution data, among others, for applications in the field of urban planning and development and urban growth assessment. However, for certain application fields and parameters, such as urban climate analysis and urban structure parameters, image fusion techniques will be valuable by enhancing the spatial resolution or extending the available information with thermal properties.

For such investigations a simulated urban EnMAP scene would be of great benefit. First simulated EnMAP data has been generated for a geological site [168] and an agricultural site [169]. They were produced by a scene simulator for optical remote sensing imageries [31] with a special emphasis on EnMAP HSI data simulation. With this, EnMAP scenes can be generated over several natural environments, acquisition and illumination geometries, cloud covers, and instrument configurations. For the simulation of an urban scene, additional BRDF effects have to be taken into account by using a high resolution surface model of the city. This enables the retrieval of surface reflectance by considering the complex radiative transfer processes due to the urban structure [122,170] and thus, helps to better understand the spectral mixture characteristics of an urban EnMAP HSI pixel.

In the future, other spaceborne imaging spectrometers are also planned, each with its own specific sensor characteristics. On the one hand, this ensures the continuity of spaceborne imaging spectroscopy data to allow long-term monitoring of urban areas in high thematic detail. On the other hand, these missions provide the opportunity for a combined analysis in the thermal (e.g., HypSPIRI) and spatial domain (e.g., HISUI). Together with these missions, the EnMAP mission can be the starting point of a new generation of high-quality sensors available for continuous global urban analysis.

Acknowledgements

This work has been carried out in the frame of the EnMAP preparation activities and is sponsored by the Space Agency of the German Aerospace Center (DLR) through funds of the Federal Ministry of Economics and Technology, following a decision of the German Federal Parliament (Grant Code 50EE0946). We wish to acknowledge the anonymous reviewers for their helpful comments.

References

1. United Nations. *World Urbanization Prospects: The 2009 Revision*; Department of Economic and Social Affairs, Population Division: New York, NY, USA, 2010; Available online: <http://esa.un.org/unpd/wup/index.htm> (accessed on 25 January 2011).
2. CEOS. *CEOS EO Handbook—Catalogue of Satellite Instruments*; ESA: Ispra, Italy, 2011; Available online: <http://database.eohandbook.com/database/instrumenttable.aspx> (accessed on 31 January 2011).
3. Ben-Dor, E.; Levin, N.; Saaroni, H. A spectral based recognition of the urban environment using the visible and near-infrared spectral region (0.4–1.1 μm). A case study over Tel-Aviv, Israel. *Int. J. Remote Sens.* **2001**, *22*, 2193–2218.
4. Heiden, U.; Segl, K.; Roessner, S.; Kaufmann, H. Determination of robust spectral features for identification of urban surface materials in hyperspectral remote sensing data. *Remote Sens. Environ.* **2007**, *111*, 537–552.
5. Herold, M.; Roberts, D.A.; Gardner, M.E.; Dennison, P.E. Spectrometry for urban area remote sensing—Development and analysis of a spectral library from 350 to 2,400 nm. *Remote Sens. Environ.* **2004**, *91*, 304–319.
6. Weng, Q.; Hu, X.; Lu, D. Extracting impervious surfaces from medium spatial resolution multispectral and hyperspectral imagery: A comparison. *Int. J. Remote Sens.* **2008**, *29*, 3209–3232.
7. Xu, B.; Gong, P. Land-use/Land-cover classification with multispectral and hyperspectral EO-1 data. *Photogramm. Eng. Remote Sensing* **2007**, *73*, 955–965.
8. Cavalli, R.M.; Fusilli, L.; Pascucci, S.; Pignatti, S.; Santini, F. Hyperspectral sensor data capability for retrieving complex urban land cover in comparison with multispectral data: Venice City case study (Italy). *Sensors* **2008**, *8*, 3299–3320.
9. Ungar, S.G.; Reuter, D.; Pearlman, J.S.; Mendenhall, J.A. Overview of the Earth Observing One (EO-1) mission. *IEEE Trans. Geosci. Remote Sens.* **2003**, *41*, 1149–1159.
10. Cutter, M.A.; Johns, L.S.; Lobb, D.R.; Williams, T.L.; Settle, J.J. Flight experience of the Compact High Resolution Imaging Spectrometer (CHRIS). *Proc. SPIE* **2004**, *5159*, 392.
11. Small, C. Spectral Dimensionality and Scale of Urban Radiance. Presented at *2001 AVIRIS Workshop*, Pasadena, CA, USA, 27 February–2 March 2001.
12. Herold, M.; Gardner, M.E.; Roberts, D.A. Spectral Resolution Requirements for Mapping Urban Areas. *IEEE Trans. Geosci. Remote Sens.* **2003**, *41*, 1907–1919.
13. Zhang, Q.; Wang, J.; Peng, X.; Gong, P.; Shi, P. Urban built-up land change detection with road density and spectral information from multi-temporal Landsat TM data. *Int. J. Remote Sens.* **2002**, *23*, 3057–3078.
14. Taubenböck, H.; Wegmann, M.; Roth, A.; Mehl, H.; Dech, S. Urbanization in India—Spatiotemporal analysis using remote sensing data. *Comput. Environ. Urban Syst.* **2009**, *33*, 179–188.

15. Orenstein, D.E.; Bradley, B.A.; Albert, J.; Mustard, J.F.; Hamburg, S.P. How much is built? Quantifying and interpreting patterns of built space from different data sources. *Int. J. Remote Sens.* **2011**, *32*, 2621–2644.
16. Jat, M.K.; Garg, P.; Khare, D. Monitoring and modelling of urban sprawl using remote sensing and GIS techniques. *Int. J. Appl. Earth Obs. Geoinf.* **2008**, *10*, 26–43.
17. Heldens, W. Use of Airborne Hyperspectral Data and Height Information to Support Urban Micro Climate Characterisation. Ph.D. Thesis, Bayerischen Julius-Maximilians Universität Würzburg, Würzburg, Germany, 2010.
18. Heiden, U.; Segl, K.; Roessner, S.; Kaufmann, H. Ecological Evaluation of Urban Biotope Types Using Airborne Hyperspectral HyMap Data. In *Proceedings of the 2nd GRSS/ISPRS Joint Workshop on Remote Sensing and Data Fusion over Urban Areas*, Berlin, Germany, 22–23 May 2003; pp. 18–22.
19. Lo, C. Applications of Landsat TM data for quality of life assessment in an urban environment. *Comput. Environ. Urban Syst.* **1997**, *21*, 259–276.
20. Lu, D.S.; Weng, Q.H. Use of impervious surface in urban land-use classification. *Remote Sens. Environ.* **2006**, *102*, 146–160.
21. Wurm, M.; Taubenböck, H.; Roth, A.; Dech, S. Urban Structuring Using Multisensoral Remote Sensing Data—By the Example of German Cities: Cologne and Dresden. In *Proceedings of Urban Remote Sensing Joint Event*, Shanghai, China, 20–22 May 2009.
22. Taubenböck, H.; Wegman, M.; Wurm, M.; Ullmann, T.; Dech, S. The Global Trend of Urbanization—Spatiotemporal Analysis of Mega Cities Using Multi-Temporal Remote Sensing, Landscape Metrics and Gradient Analysis. In *Proceedings of SPIE's International Symposium, Remote Sensing Europe*, Toulouse, France, 20–23 September 2010.
23. Inglada, J. Automatic recognition of man-made objects in high resolution optical remote sensing images by SVM classification of geometric image features. *ISPRS J. Photogramm.* **2007**, *62*, 236–248.
24. Roessner, S.; Segl, K.; Heiden, U.; Kaufmann, H. Automated differentiation of urban surfaces based on airborne hyperspectral imagery. *IEEE Trans. Geosci. Remote Sens.* **2001**, *39*, 1525–1532.
25. Kawashima, T.; Narimatsu, Y.; Inada, H.; Ishida, J.; Hamada, K.; Ito, Y.; Yoshida, J.; Ohgi, N.; Tatsumi, K.; Harada, H.; Kawanishi, T.; Sakuma, F.; Iwasaki, A. The functional evaluation model for the on-board hyperspectral radiometer. *Proc. SPIE* **2010**, 7857, 78570M.
26. Green, R.; Asner, G.; Ungar, S.; Knox, R. NASA Mission to Measure Global Plant Physiology and Functional Types. In *Proceedings of 2008 IEEE Aerospace Conference*, Big Sky, MT, USA, 1–8 March 2008.
27. Kaufmann, H.; Segl, K.; Chabrillat, S.; Hofer, S.; Stuffer, T.; Müller, A.; Richter, R.; Schreier, G.; Haydn, R.; Bach, H. A Hyperspectral Sensor for Environmental Mapping and Analysis. In *Proceedings of IEEE International Geoscience and Remote Sensing Symposium (IGARSS 2006) & 27th Canadian Symposium on Remote Sensing*, Denver, CO, USA, 31 July–4 August 2006.

28. Matsunaga, T.; Iwasaki, A.; Kahimura, O.; Ogawa, K.; Ohgi, N.; Tsuchida, S. HISUI—Hyperspectral Imager Suite. A Japanese Spaceborne Hyperspectral and Multispectral Remote Sensing Mission. Presented at *HyspIRI Science Workshop*, Pasadena, CA, USA, 24–26 August 2010.
29. Staenz, K. Terrestrial Imaging Spectroscopy Some Future Perspectives. In *Proceedings of 6th EARSeL Workshop on Imaging Spectroscopy*, Tel-Aviv, Israel, 16–19 March 2009.
30. Mogulsky, V.; Hofer, S.; Sang, B.; Schubert, J.; Stuffer, T.; Müller, A.; Chlebek, C.; Kaufmann, H. EnMAP Hyperspectral Imaging Sensor On-Board Calibration Approach. In *Proceedings of 6th EARSeL Workshop on Imaging Spectroscopy*, Tel-Aviv, Israel, 16–19 March 2009.
31. Guanter, L.; Segl, K.; Kaufmann, H. Simulation of the optical remote-sensing scenes with application to the EnMAP hyperspectral mission. *IEEE Trans. Geosci. Remote Sens.* **2009**, *47*, 2340–2351.
32. Stuffer, T.; Kaufmann, C.; Hofer, S.; Förster, K.P.; Schreier, G.; Mueller, A.; Eckardt, A.; Bach, H.; Penné, B.; Benz, U.; Haydn, R. The EnMAP hyperspectral imager. An advanced optical payload for future applications in Earth observation programmes. *Acta Astronautica* **2007**, *61*, 115–120.
33. EnMAP Hyperspectral Imager (HSI). Available online: www.enmap.org/sensors (accessed on 31 May 2011).
34. Van der Linden, S.; Rabe, A.; Leitão, P.; Hostert, P. Die EnMAP-Box: Ziele, Stand der Entwicklung und Ausblick. Presented at *Nationaler EnMAP-Workshop 2010*, Berlin, Germany, 25 October 2010; Available online: http://www.enmap.org/sites/enmap/files/documentation/events/2nd_WS_Potsdam/Vortraege/allgemein_enmap-box_van%20der%20linden.pdf (accessed on 21 February 2011).
35. Wende, W.; Huelsmann, W.; Marty, M.; Penn-Bressel, G.; Bobylev, N. Climate protection and compact urban structures in spatial planning and local construction plans in Germany. *Land Use Policy* **2010**, *27*, 864–868.
36. Banzhaf, E.; Hofer, R. Monitoring urban structure types as spatial indicators with CIR aerial photographs for a more effective urban environmental management. *IEEE J. Sel. Topics Appl. Earth Obs. Remote Sens.* **2008**, *1*, 129–138.
37. Haala, N.; Brenner, C. Extraction of buildings and trees in urban environments. *ISPRS J. Photogramm.* **1999**, *54*, 130–137.
38. Guo, L.; Chehata, N.; Mallet, C.; Boukir, S. Relevance of airborne lidar and multispectral image data for urban scene classification using Random Forests. *ISPRS J. Photogramm.* **2011**, *66*, 56–66.
39. Lu, D.; Weng, Q. A survey of image classification methods and techniques for improving classification performance. *Int. J. Remote Sens.* **2007**, *28*, 823–870.
40. Zha, Y.; Gao, J.; Ni, S. Use of normalized difference built-up index in automatically mapping urban areas from TM imagery. *Int. J. Remote Sens.* **2003**, *24*, 583–594.

41. Esch, T.; Himmler, V.; Schorcht, G.; Thiel, M.; Wehrmann, T.; Bachofer, F.; Conrad, C.; Schmidt, M.; Dech, S. Large-area assessment of impervious surface based on integrated analysis of single-date Landsat-7 images and geospatial vector data. *Remote Sens. Environ.* **2009**, *113*, 1678–1690.
42. Small, C. Estimation of urban vegetation abundance by spectral mixture analysis. *Int. J. Remote Sens.* **2001**, *22*, 1305–1334.
43. Huang, J.; Lu, X.; Sellers, J.M. A global comparative analysis of urban form: Applying spatial metrics and remote sensing. *Landscape Urban Plan.* **2007**, *82*, 184–197.
44. Hasse, J.; Lathrop, R. A Housing-Unit-Level approach to characterizing residential sprawl. *Photogramm. Eng. Remote Sensing* **2003**, *69*, 1021–1030.
45. Schneider, A.; Friedl, M.A.; Potere, D. Mapping global urban areas using MODIS 500-m data: New methods and datasets based on ‘urban ecoregions’. *Remote Sens. Environ.* **2010**, *114*, 1733–1746.
46. Zhang, X.; Zhong, T.; Feng, X.; Wang, K. Estimation of the relationship between vegetation patches and urban land surface temperature with remote sensing. *Int. J. Remote Sens.* **2009**, *30*, 2105–2118.
47. Jain, S.; Jain, R.K. A remote sensing approach to establish relationships among different land covers at the micro level. *Int. J. Remote Sens.* **2006**, *27*, 2667–2682.
48. Heldens, W.; Esch, T.; Heiden, U.; Müller, A.; Dech, S. Exploring the Demands on Hyperspectral Data Products for Urban Planning: A Case Study in the Munich Region. In *Proceedings of the 6th EARSeL Imaging Spectroscopy SIG Workshop*, Tel Aviv, Israel, 16–19 March 2009.
49. Bochow, M.; Segl, K.; Kaufmann, H. Automating the Build-up Process of Feature-based Fuzzy Logic Models for the Identification of Urban Biotopes from Hyperspectral Remote Sensing Data. In *Proceedings of Urban Remote Sensing Joint Event*, Paris, France, 11–13 April 2007.
50. Madhavan, B.B.; Kubo, S.; Kurisaki, N.; Sivakumar, T.V.L.N. Appraising the anatomy and spatial growth of the Bangkok Metropolitan area using a vegetation-impervious-soil model through remote sensing. *Int. J. Remote Sens.* **2001**, *22*, 789–806.
51. Jat, M.K.; Garg, P.K.; Khare, D. Modelling of urban growth using spatial analysis techniques: A case study of Ajmer city (India). *Int. J. Remote Sens.* **2008**, *29*, 543–567.
52. Banzhaf, E.; Grescho, V.; Kindler, A. Monitoring urban to peri-urban development with integrated remote sensing and GIS information: A Leipzig, Germany case study. *Int. J. Remote Sens.* **2009**, *30*, 1675–1696.
53. Griffiths, P.; Hostert, P.; Gruebner, O.; Van der Linden, S. Mapping megacity growth with multi-sensor data. *Remote Sens. Environ.* **2010**, *114*, 426–439.
54. Durieux, L.; Lagabrielle, E.; Nelson, A. A method for monitoring building construction in urban sprawl areas using object-based analysis of Spot 5 images and existing GIS data. *ISPRS J. Photogramm.* **2008**, *63*, 399–408.
55. Bochow, M.; Segl, K.; Kaufmann, H. An Update System for Urban Biotope Maps Based on Hyperspectral Remote Sensing Data. In *Proceedings of 5th EARSeL Workshop on Imaging Spectroscopy*, Bruges, Belgium, 23–25 April 2007.

56. Taubenböck, H.; Post, J.; Roth, A.; Zosseder, K.; Struntz, G.; Dech, S. A conceptual vulnerability and risk framework as outline to identify capabilities of remote sensing. *Natural Hazards Earth Syst. Sci.* **2008**, *8*, 409–420.
57. Dousset, B.; Gourmelon, F.; Mauri, E. Application of satellite Remote Sensing for Urban Risk Analysis: A Case Study of the 2003 Extreme Heat Wave in Paris. In *Proceedings of Urban Remote Sensing Joint Event*, Paris, France, 11–13 April 2007; pp. 1–5.
58. Clark, R.; Green, R.; Swayze, G.; Sutley, S.; Hoefen, T.; Livo, K.E.; Plumlee, G.; Pavri, B.; Sarture, C.; Wilson, S.; Hageman, P.; Lamothe, P.; Vance, J.; Boardman, J.; Brownfield, I.; Gent, C.; Morath, L.; Taggart, J.; Theodorakos, P.; Adams, M. *Environmental Studies of the World Trade Centre Area after the September 11, 2001 Attack*; Open File Report OFR-01-0429; US Geological Survey: Denver, CO, USA, 2001.
59. Bassani, C.; Cavalli, R.M.; Cavalcante, F.; Cuomo, V.; Palombo, A.; Pascucci, S.; Pignatti, S. Deterioration status of asbestos-cement roofing sheets assessed by analyzing hyperspectral data. *Remote Sens. Environ.* **2007**, *109*, 361–378.
60. Stefanov, W.L.; Netzband, M. Assessment of ASTER land cover and MODIS NDVI data at multiple scales for ecological characterization of an and urban center. *Remote Sens. Environ.* **2005**, *99*, 31–43.
61. Zhang, Y.; Odeh, I.O.; Han, C. Bi-temporal characterization of land surface temperature in relation to impervious surface area, NDVI and NDBI, using a sub-pixel image analysis. *Int. J. Appl. Earth Obs. Geoinf.* **2009**, *11*, 256–264.
62. Yuan, F.; Bauer, M.E. Comparison of impervious surface area and normalized difference vegetation index as indicators of surface urban heat island effects in Landsat imagery. *Remote Sens. Environ.* **2007**, *106*, 375–386.
63. Xu, W.; Wooster, M.; Grimmond, C. Modelling of urban sensible heat flux at multiple spatial scales: A demonstration using airborne hyperspectral imagery of Shanghai and a temperature-emissivity separation approach. *Remote Sens. Environ.* **2008**, *112*, 3493–3510.
64. Wu, C. Quantifying high-resolution impervious surfaces using spectral mixture analysis. *Int. J. Remote Sens.* **2009**, *30*, 2915–2932.
65. Van de Voorde, T.; De Roeck, T.; Canters, F. A comparison of two spectral mixture modelling approaches for impervious surface mapping in urban areas. *Int. J. Remote Sens.* **2009**, *30*, 4785–4806.
66. Pauleit, S.; Duhme, F. Assessing the environmental performance of land cover types for urban planning. *Landscape Urban Plan.* **2000**, *52*, 1–20.
67. Sukkopp, H.; Wittig, R. *Stadtökologie. Ein Fachbuch für Studium und Praxis*, 2ed.; Gustav Fischer: Stuttgart, Germany, 1998.
68. Herold, M.; Liu, X.; Clarke, K.C. Spatial metrics and image texture for mapping urban land use. *Photogramm. Eng. Remote Sensing* **2003**, *69*, 991–1001.
69. Pacifici, F.; Chini, M.; Emery, W. A neural network approach using multi-scale textural metrics from very high-resolution panchromatic imagery for urban land-use classification. *Remote Sens. Environ.* **2009**, *113*, 12761292.

70. Tuia, D.; Pacifici, F.; Kanevski, M.; Emery, W. Classification of Very High Spatial Resolution Imagery using mathematical morphology and support vector machines. *IEEE Trans. Geosci. Remote Sens.* **2009**, *47*, 3866–3879.
71. Goebel, J.; Wurm, M.; Wagner, G. *Exploring the Linkage of Spatial Indicators from Remote Sensing Data with Survey Data—The Case of the Socio-Economic Panel (SOEP) and 3D City Models*; SOEPpapers 283; DIW Berlin: Berlin, Germany, 2010; p. 14.
72. Zhou, W.; Troy, A. An object-oriented approach for analysing and characterizing urban landscape at the parcel level. *Int. J. Remote Sens.* **2008**, *29*, 3119–3135.
73. Pesaresi, M.; Gerhardinger, A.; Kayitakire, F. A robust built-up ree Presence Index by anisotropic rotation-invariant textural measure. *IEEE J. Appl. Earth Obs. Remote Sens.* **2008**, *1*, 180–192.
74. Pesaresi, M.; Gerhardinger, A.; Kayitakire, F. Monitoring Settlement Dynamics by Anisotropic Textural Analysis of Panchromatic VHR Data. In *Proceedings of the 2007 Urban Remote Sensing Joint Event URBAN2007-URS2007*, Paris, France, 11–13 April 2007.
75. Gluch, R. Urban growth detection using texture analysis on merged Landsat TM and SPOT-P data. *Photogramm. Eng. Remote Sensing* **2002**, *68*, 1283–1288.
76. Kurtz, C.; Passat, N.; Ganarski, P.; Puissant, A. Multi-resolution region-based clustering for urban analysis. *Int. J. Remote Sens.* **2010**, *31*, 5941–5973.
77. Lu, D.; Moran, E.; Hetrick, S. Detection of impervious surface change with multitemporal Landsat images in an urban-rural frontier. *ISPRS J. Photogramm.* **2011**, *66*, 298–306.
78. Weng, Q.; Hu, X.; Liu, H. Estimating impervious surfaces using linear spectral mixture analysis with multitemporal ASTER images. *Int. J. Remote Sens.* **2009**, *30*, 4807–4830.
79. Elmore, A.J.; Guinn, S.M. Synergistic use of Landsat Multispectral Scanner with GIRAS land-cover data to retrieve impervious surface area for the Potomac River Basin in 1975. *Remote Sens. Environ.* **2010**, *114*, 2384–2391.
80. Martinuzzi, S.; Gould, W.A.; Ramos Gonzalez, O.M. Land development, land use, and urban sprawl in Puerto Rico integrating remote sensing and population census data. *Landscape. Urban Plan.* **2007**, *79*, 288–297.
81. Khatsu, P.; van Westen, C. Urban Multi-Hazard Risk Analysis Using GIS and Remote Sensing: A Case Study from Kohima Town, Nagaland, India. In *Proceedings of the 26th Asian Conference on Remote Sensing*, Hanoi, Vietnam, 7–11 November 2005.
82. Bhaskaran, S.; Datt, B.; Forster, B.; Neal, T.; Brown, M. Integrating imaging spectroscopy (445–2543 nm) and geographic information systems for post-disaster management: A case of hailstorm damage in Sydney. *Int. J. Remote Sens.* **2004**, *25*, 2625–2639.
83. Voigt, S.; Kemper, T.; Riedlinger, T.; Kiefl, R.; Scholte, K.; Mehl, H. Satellite image analysis for disaster and crisis-management support. *IEEE Trans. Geosci. Remote Sens.* **2007**, *45*, 1520–1528.
84. Ajmar, A.; Boccardo, P.; Tonolo, F.; Veloso, C. Earthquake damage assessment using remote sensing imagery. The Haiti case study. In *Geoinformation for Disaster and Risk Management: Examples and Best Practices*; Altan, O., Backhaus, R., Boccardo, P., Zlatanova, S., Eds; Joint Board of Geospatial Information Societies: Copenhagen, Denmark, 2010; pp. 31–38.

85. Wegscheider, S.; Post, J. *Satellite-Based Crisis Information and Risk Assessment: Contributions Following the Earthquake in W. Sumatra and the Mentawai Tsunami*; 2 March 2011.
86. Marino, A.; Ludovisi, G.; Moccaldi, A.; Damiani, F. Hyperspectral remote sensing and GIS techniques application for the evaluation and monitoring of interactions between natural risks and industrial hazards. *Proc. SPIE* **2001**, *4151*, 231–236.
87. Voogt, J.A.; Oke, T.R. Thermal remote sensing of urban climates. *Remote Sens. Environ.* **2003**, *86*, 370–384.
88. Chen, X.L.; Zhao, H.M.; Li, P.X.; Yin, Z.Y. Remote sensing image-based analysis of the relationship between urban heat island and land use/cover changes. *Remote Sens. Environ.* **2006**, *104*, 133–146.
89. Xian, G. Satellite remotely-sensed land surface parameters and their climatic effects for three metropolitan regions. *Adv. Space Res.* **2008**, *41*, 1861–1869.
90. Jenerette, G.D.; Harlan, S.L.; Brazel, A.; Jones, N.; Larsen, L.; Stefanov, W.L. Regional relationships between surface temperature, vegetation, and human settlement in a rapidly urbanizing ecosystem. *Landscape Ecol.* **2007**, *22*, 353–365.
91. Weng, Q.; Lu, D.; Schubring, J. Estimation of land surface temperature-vegetation abundance relationship for urban heat island studies. *Remote Sens. Environ.* **2004**, *89*, 467–483.
92. Pena, M.A. Relationships between remotely sensed surface parameters associated with the urban heat sink formation in Santiago, Chile. *Int. J. Remote Sens.* **2008**, *29*, 4385–4404.
93. Hoyano, A.; Iino, A.; Ono, M.; Taniguchi, S. Analysis of the influence of urban form and materials on sensible heat flux—A case study of Japan’s largest housing development ‘Tama New Town’. *Atmos. Environ.* **1999**, *33*, 3931–3939.
94. Jung, A.; Tökei, L.; Kardeván, P. Application of airborne hyperspectral and thermal images to analyse urban microclimate. *Appl. Ecol. Environ. Res.* **2007**, *5*, 165–175.
95. Heldens, W.; Heiden, U.; Esch, T.; Dech, S. Potential of Hyperspectral Data for Urban Micro Climate Analysis. In *Proceedings of the Hyperspectral Workshop 2010*, Frascati, Italy, 17–19 March 2010; p. 8.
96. Frey, C.; Rigo, G.; Parlow, E. Urban radiation balance of two coastal cities in a hot and dry environment. *Int. J. Remote Sens.* **2007**, *28*, 2695–2712.
97. Govaerts, Y.; Lattanzio, A.; Taberner, M.; Pinty, B. Generating global surface albedo products from multiple geostationary satellites. *Remote Sens. Environ.* **2008**, *112*, 2804–2816.
98. Weng, Q.; Lu, D. Landscape as a continuum: An examination of the urban landscape structures and dynamics of Indianapolis City, 1991–2000, by using satellite images. *Int. J. Remote Sens.* **2009**, *30*, 2547–2577.
99. Roessner, S.; Segl, K.; Bochow, M.; Heiden, U.; Heldens, W.; Kaufmann, H. Potential of hyperspectral remote sensing for analyzing the urban environment. In *Urban Remote Sensing: Monitoring, Synthesis and Modeling in the Urban Environment*; Yang, X., Ed.; Wiley-Blackwell: Chichester, UK, 2011.
100. Anderson, J.R.; Hardy, E.E.; Roach, J.T.; Witmer, R.E. *A Land Use and Land Cover Classification Scheme for Use with Remote Sensor Data*; Professional Paper 964; US GPO: Washington, DC, USA, 1976.

101. Ridd, M.K. Exploring a V-I-S (Vegetation-Impervious Surface-Soil) model for urban ecosystem analysis through remote sensing—Comparative anatomy for cities. *Int. J. Remote Sens.* **1995**, *16*, 2165–2185.
102. Wu, C.; Murray, A.T. Estimating impervious surface distribution by spectral mixture analysis. *Remote Sens. Environ.* **2003**, *84*, 493–505.
103. Gluch, R.; Quattrochi, D.A.; Luvall, J.C. A multi-scale approach to urban thermal analysis. *Remote Sens. Environ.* **2006**, *104*, 123–132.
104. Small, C. High spatial resolution spectral mixture analysis of urban reflectance. *Remote Sens. Environ.* **2003**, *88*, 170–186.
105. Powell, R.L.; Roberts, D.A.; Dennison, P.E.; Hess, L.L. Sub-pixel mapping of urban land cover using multiple endmember spectral mixture analysis: Manaus, Brazil. *Remote Sens. Environ.* **2007**, *106*, 253–267.
106. Phinn, S.; Stanford, M.; Scarth, P.; Murray, A.T.; Shyy, P.T. Monitoring the composition of urban environments based on the vegetation-impervious surface-soil (VIS) model by subpixel analysis techniques. *Int. J. Remote Sens.* **2002**, *23*, 4131–4153.
107. Small, C.; Lu, J.W. Estimation and vicarious validation of urban vegetation abundance by spectral mixture analysis. *Remote Sens. Environ.* **2006**, *100*, 441–456.
108. Chen, X.; Li, L. A comparison of spectral mixture analysis methods for urban landscape using landsat ETM+ data: Los Angeles, CA. In *The International Archives of the Photogrammetry, Remote Sensing and Spatial Information Sciences*; 2008; Volume XXXVII, Part B7, pp. 635–639.
109. Wentz, E.A.; Nelson, D.; Rahman, A.; Stefanov, W.L.; Roy, S.S. Expert system classification of urban land use/cover for Delhi, India. *Int. J. Remote Sens.* **2008**, *29*, 4405–4427.
110. Berberoglu, S.; Lloyd, C.; Atkinson, P.; Curran, P. The integration of spectral and textural information using neural networks for land cover mapping in the Mediterranean. *Comput. Geosci.* **2000**, *26*, 385–396.
111. Song, M.; Civco, D.L.; Hurd, J.D. A competitive pixel-object approach for land cover classification. *Int. J. Remote Sens.* **2005**, *26*, 4981–4997.
112. Pu, R.; Gong, P.; Michishita, R.; Sasagawa, T. Spectral mixture analysis for mapping abundance of urban surface components from the Terra/ASTER data. *Remote Sens. Environ.* **2008**, *112*, 939–954.
113. Su, W.; Li, J.; Chen, Y.; Liu, Z.; Zhang, J.; Low, T.M.; Suppiah, I.; Hashim, S.A.M. Textural and local spatial statistics for the object-oriented classification of urban areas using high resolution imagery. *Int. J. Remote Sens.* **2008**, *29*, 3105–3117.
114. Tarabalka, Y.; Chanussot, J.; Benediktsson, J.A. Spectral-spatial classification of hyperspectral images using segmentation-derived adaptive neighborhoods. In *Multivariate Image Processing*; Collet, C., Chanussot, J., Chendi, K., Eds.; ISTE Ltd and John Wiley & Sons Inc.: Hoboken, NJ, USA, 2009; pp. 341–374.
115. Schaepman, M.E.; Ustin, S.L.; Plaza, A.J.; Painter, T.H.; Verrelst, J.; Liang, S. Earth system science related imaging spectroscopy—An assessment. *Remote Sens. Environ.* **2009**, *113* (Suppl. 1), S123–S137.

116. Van der Meer, F.; de Jong, S.M. *Imaging Spectrometry*; Springer: Dordrecht, The Netherlands, 2003.
117. Herold, M.; Roberts, D. Spectral characteristics of asphalt road aging and deterioration: Implications for remote-sensing applications. *Appl. Opt.* **2005**, *44*, 4327–4334.
118. Lacherade, S.; Miesch, C.; Briottet, X.; Le Men, H. Spectral variability and bidirectional reflectance behaviour of urban materials at a 20 cm spatial resolution in the visible and near-infrared wavelengths. A case study over Toulouse (France). *Int. J. Remote Sens.* **2005**, *26*, 3859 – 3866.
119. Feingersh, T.; Ben-Dor, E.; Portugali, J. Construction of synthetic spectral reflectance of remotely sensed imagery for planning purposes. *Environ. Modell. Softw.* **2007**, *22*, 335–348.
120. Meister, G.; Rothkirch, A.; Spitzer, H.; Bienlein, J.K. Large-scale bidirectional reflectance model for urban areas. *IEEE Trans. Geosci. Remote Sens.* **2001**, *39*, 1927–1942.
121. Bochow, M.; Rogass, C.; Segl, K.; Kaufmann, H. Automatic Shadow Detection in Hyperspectral VIS-NIR Images. In *Proceedings of the 7th EARSeL Workshop of the Special Interest Group in Imaging Spectroscopy*, Edinburgh, UK, 11–13 April 2011.
122. Richter, R.; Müller, A. De-shadowing of satellite/airborne imagery. *Int. J. Remote Sens.* **2005**, *26*, 3137–3148.
123. Dell’Acqua, F.; Gamba, P.; Trianni, G. A Preliminary Study on Separability of Paving Materials in Shadowed Hyperspectral Pixels from a Central Urban Area. In *Proceedings of ISPRS Joint Conferences: 3rd International Symposium Remote Sensing and Data Fusion Over Urban Areas (URBAN 2005) and 5th International Symposium Remote Sensing of Urban Areas (URS 2005)*, Tempe, AZ, USA, 14–16 March 2005.
124. Hughes, G. On the mean accuracy of statistical pattern recognizers. *IEEE Trans. Inf. Theory* **1968**, *14*, 55–63.
125. Van der Meer, F. The effectiveness of spectral similarity measures for the analysis of hyperspectral imagery. *Int. J. Appl. Earth Obs. Geoinf.* **2006**, *8*, 3–17.
126. Bue, B.; Merenyi, E.; Csatho, B. Automated labeling of materials in hyperspectral imagery. *IEEE Trans. Geosci. Remote Sens.* **2010**, *48*, 4059 –4070.
127. Chang, C. An information theoretic-based approach to spectral variability, similarity and discriminability for hyperspectral image analysis. *IEEE Trans. Inf. Theory* **2000**, *46*, 1927–1932.
128. Kruse, F.; Lefkoff, A.; Boardman, J.; Heidebrecht, K.; Shapiro, A.; Barloon, P.; Goetz, A. The spectral image processing system (SIPS)—Interactive visualization and analysis of imaging spectrometer data. *Remote Sens. Environ.* **1993**, *44*, 145–163.
129. Chen, J.; Hepner, G.F. Investigation of Imaging Spectroscopy for Discriminating Urban Land Covers and Surface Materials. Presented at *AVIRIS Workshop Proceedings*, Pasadena, CA, USA, 27 February–2 March 2001.
130. Clark, R.; Gallagher, A.; Swayze, G. Material Absorption Band Depth Mapping of Imaging Spectrometer Data Using a Complete Band Shape Least-Squares Fit with Library Reference Spectra. In *Proceedings of the 2nd AVIRIS Earth Science Workshop*, Pasadena, CA, USA, 4–5 June 1990.

131. Clark, R.N.; Swayze, G.A.; Livo, K.E.; Kokaly, R.F.; Sutley, S.J.; Dalton, J.B.; McDougal, R.R.; Gent, C.A. Imaging spectroscopy: Earth and planetary remote sensing with the USGS Tetracorder and expert systems. *J. Geophys. Res.: Planets* **2003**, *108*, 5131.
132. Yang, H.; Ma, B.; Du, Q.; Yang, C. Improving urban land use and land cover classification from high-spatial-resolution hyperspectral imagery using contextual information. *J. Appl. Remote Sens.* **2010**, *4*, 041890.
133. Van der Linden, S.; Janz, A.; Waske, B.; Eiden, M.; Hostert, P. Classifying segmented hyperspectral data from a heterogeneous urban environment. *J. Appl. Remote Sens.* **2007**, *1*, 013543.
134. Bruzzone, L.; Carlin, L. A multilevel context-based system for classification of very high spatial resolution images. *IEEE Trans. Geosci. Remote Sens.* **2006**, *44*, 2587–2600.
135. Plaza, A.; Benediktsson, J.A.; Boardman, J.W.; Brazile, J.; Bruzzone, L.; Camps-Valls, G.; Chanussot, J.; Fauvel, M.; Gamba, P.; Gualtieri, A.; Marconcini, M.; Tilton, J.C.; Trianni, G. Recent advances in techniques for hyperspectral image processing. *Remote Sens. Environ.* **2009**, *113 (Suppl. 1)*, S110–S122.
136. Adams, J.; Smith, M.; Gillespie, A. Imaging spectroscopy: Interpretation based on spectral mixture analysis. In *Remote Geochemical Analysis: Elemental and Mineralogical Composition*; Pieters, C., Englert, P., Eds.; Cambridge University Press: New York, NY, USA, 1993; pp. 145–166.
137. Segl, K.; Roessner, S.; Heiden, U.; Kaufmann, H. Fusion of spectral and shape features for identification of urban surface cover types using reflective and thermal hyperspectral data. *ISPRS J. Photogramm.* **2003**, *58*, 99–112.
138. Franke, J.; Roberts, D.A.; Halligan, K.; Menz, G. Hierarchical Multiple Endmember Spectral Mixture Analysis (MESMA) of hyperspectral imagery for urban environments. *Remote Sens. Environ.* **2009**, *113*, 1678–1690.
139. Somers, B.; Asner, G.P.; Tits, L.; Coppin, P. Endmember variability in Spectral Mixture Analysis: A review. *Remote Sens. Environ.* **2011**, *115*, 1603–1616.
140. Rogge, D.; Rivard, B.; Zhang, J.; Harris, J.; Sanchez, A.; Feng, J. Integration of spatial-spectral information for the improved extraction of endmembers. *Remote Sens. Environ.* **2007**, *110*, 287–303.
141. Roberts, D.; Gardner, M.; Church, R. Mapping chaparral in the Santa Monica Mountains using multiple endmember spectral mixture analysis. *Remote Sens. Environ.* **1998**, *65*, 267–279.
142. Borel, C.; Ewald, K.; Manzardo, M.; Wamsley, C.; Jacobson, J. Adjoint Radiosity Based Algorithms for Retrieving Target Reflectances in Urban Area Shadows. In *Proceedings of the 6th EARSeL Imaging Spectroscopy SIG Workshop*, Tel Aviv, Israel, 16–19 March 2009.
143. Keshava, N. A Survey of Spectral Unmixing Algorithms. *Lincoln Laboratory J.* **2003**, *14*, 55–78.
144. Keshava, N.; Mustard, J. Spectral unmixing. *IEEE Sign. Proc. Mag.* **2002**, *19*, 44–57.
145. Benediktsson, J.; Palmason, J.; Sveinsson, J.; Chanussot, J. Decision Level Fusion in Classification of Hyperspectral Data from Urban Areas. In *Proceedings of International Geoscience and Remote Sensing Symposium (IGARSS)*, Anchorage, AK, USA, 20–24 September 2004; Volume 1, pp. 73–76.

146. Plaza, A.; Martinez, P.; Perez, R.; Plaza, J. A new approach to mixed pixel classification of hyperspectral imagery based on extended morphological profiles. *Pattern Recog.* **2004**, *37*, 1097–1116.
147. Lizarazo, I. SVM-based segmentation and classification of remotely sensed data. *Int. J. Remote Sens.* **2008**, *29*, 7277–7283.
148. Kirkland, L.; Kenneth, C.; Salisbury, J. Thermal infrared spectral band detection limits for unidentified surface materials. *Appl. Opt.* **2001**, *40*, 4852–4864.
149. Müller, A.; Richter, R.; Habermeyer, M.; Dech, S.; Segl, K.; Kaufmann, H. Spectroradiometric requirements for the reflective module of the airborne spectrometer ARES. *IEEE Geosci. Remote Sens. Lett.* **2005**, *2*, 329–332.
150. Kirkland, L.; Herr, K.; Adams, P. Infrared stealthy surfaces: Why TES and THEMIS may miss some substantial mineral deposits on Mars and implications for remote sensing of planetary surfaces. *J. Geophys. Res.* **2003**, *108*, 5137.
151. Sukopp, H.; Weiler, S. Biotope mapping and nature conservation strategies in urban areas of the Federal Republic of Germany. *Landscape Urban Plan.* **1988**, *15*, 39 – 58.
152. Heiden, U.; Heldens, W.; Roessner, R.; Segl, K.; Esch, T.; Mueller, A. Imaging spectroscopy for the characterization of urban structures. *Landscape Urban Plan.* **2011**, submitted.
153. Bochow, M.; Taubenböck, H.; Segl, K.; Kaufmann, H. An Automated and Adaptable Approach for Characterizing and Partitioning Cities into Urban Structure Types. In *Proceedings of IGARSS' 2010*, Honolulu, HI, USA, 25–30 July 2010; pp. 1796–1799.
154. Mende, A.; Heiden, U.; Bachmann, M.; Hoja, D.; Buchroithner, M. Development of a New Spectral Library Classifier for Airborne Hyperspectral Images on Heterogeneous Environments. In *Proceedings of the 7th EARSeL Workshop of the Special Interest Group in Imaging Spectroscopy*, Edinburgh, UK, 11–13 April 2011.
155. Barducci, A.; Guzzi, D.; Marcoionni, P.; Pippi, I. Investigating the angular and spectral properties of natural targets using CHRIS-PROBA images of San Rossore test site. *Int. J. Remote Sens.* **2009**, *30*, 533–553.
156. Rautiainen, M.; Lang, M.; Mottus, M.; Kuusk, A.; Nilson, T.; Kuusk, J.; Lukk, T. Multi-angular reflectance properties of a hemiboreal forest: An analysis using CHRIS PROBA data. *Remote Sens. Environ.* **2008**, *112*, 2627–2642.
157. Schill, S.R.; Jensen, J.R.; Raber, G.T.; Porter, D.E. Temporal modelling of bidirectional reflectance distribution function (BRDF) in coastal vegetation. *GISci. Remote Sens.* **2004**, *41*, 116–135.
158. Meister, G.; Rothkirch, A.; Wiemker, R.; Bienlein, J.; Spitzer, H. Modeling the directional reflectance (BRDF) of a corrugated roof and experimental verification. In *Proceedings of the International Geoscience and Remote Sensing Symposium*, Seattle, WA, USA, 6–10 July 1998.
159. Meister, G. Bidirectional Reflectance of Urban Surfaces. Ph.D. Thesis, Fachbereich Physik der Universität Hamburg, Hamburg, Germany, 2000.
160. Zhang, J. Multi-source remote sensing data fusion: Status and trends. *Int. J. Image Data Fusion* **2010**, *1*, 5–24.

161. Ehlers, M.; Klonus, S.; Johan, R.P.; Rosso, P. Multi-sensor image fusion for pansharpening in remote sensing. *Int. J. Image Data Fusion* **2010**, *1*, 25–45.
162. Ehlers, M.; Klonus, S. Erhalt der spektralen Charakteristika bei der Bildfusion durch FFT basierte Filterung. *Photogrammetrie-Fernerkundung-Geoinformation* **2004**, *6*, 495–506.
163. Ehlers, M. Segment Based Image Analysis and Image Fusion. In *Proceedings of ASPRS 2007 Annual Conference*, Tampa, FL, USA, 7–11 May 2007.
164. Palubinskas, G.; Reinartz, P. Multi-Resolution, Multi-Sensor Image Fusion: General Fusion Framework. In *Proceedings of Joint Urban Remote Sensing Event JURSE*, Munich, Germany, 11–13 April 2011.
165. Eismann, M.T.; Hardie, R. Hyperspectral Resolution Enhancement Using High-Resolution Multispectral Imagery With Arbitrary Response Functions. *IEEE Trans. Geosci. Remote Sens.* **2005**, *43*, 455–465.
166. Zhukov, B.; Oertel, D.; Lanzl, F.; Reinhäckel, G. Unmixing-based multisensor multiresolution image fusion. *IEEE Trans. Geosci. Remote Sens.* **1999**, *37*, 1212–1226.
167. Oke, T. The urban energy balance. *Progr. Phys. Geogr.* **1988**, *12*, 471–508.
168. Segl, K.; Guanter, L.; Kaufmann, H.; Schubert, J.; Kaiser, S.; Sang, B.; Hofer, S. Simulation of spatial sensor characteristics in the context of the EnMAP hyperspectral mission. *IEEE Trans. Geosci. Remote Sens.* **2010**, *48*, 3046–3054.
169. Migdall, S.; Bach, H.; Kaufmann, H. Simulation of EnMAP-like Hyperspectral Images Based on Textural Information and Radiative Transfer Approach. In *Proceedings of the Hyperspectral Workshop*, Frascati, Italy, 17–19 March 2010.
170. Lacherade, S.; Miesch, C.; Boldo, D.; Briotte, X.; Valorge, C.; Le Men, H. ICARE: A physically-based model to correct atmospheric and geometric effects from high spatial and spectral remote sensing images over 3D urban areas. *Meteorol. Atmos. Phys.* **2008**, *102*, 209–222.